Cell Biol Toxicol 2007; **23:** 201–220.
DOI: 10.1007/s10565-006-0165-2

The effects of benzene exposure on apoptosis in epithelial lung cells: Localization by terminal deoxynucleotidyl transferase-mediated dUTP-biotin nick end labeling (TUNEL) and the immunocytochemical localization of apoptosis-related gene products

C.V. Weaver[1,2], S.-P. Liu[1], J.-F. Lu[2] and B.-S. Lin[2]
[1]*Department of Public Health, College of Medicine,* [2]*School of Medicine, Fu Jen University, Taipei, Taiwan, Republic of China*

Received 21 August 2006; accepted 25 October 2006; Published online: 14 December 2006

Keywords: apoptosis, benzene, carcinogenesis, genotoxicity, lung, TUNEL

Abstract

Although benzene, a well-known human carcinogen, has been shown to induce apoptosis *in vitro*, no studies have been carried out to confirm and characterize its role in activating apoptosis *in vivo*. The present study investigated the effects of benzene inhalation on the epithelial cells lining the respiratory tract including bronchioles, terminal bronchioles, respiratory bronchioles and alveoli of male Sprague-Dawley rats. Inhalation of benzene 300 ppm for 7 days induced apoptotic changes in the parenchymal components in the lung that significantly exceeded the events of programmed cell death in normal control tissues. Apoptosis was confirmed by the electrophoretic analysis of internucleosomal DNA fragmentation of benzene-exposed lung tissues, which exhibited 180–200 bp laddering subunits indicative of genomic DNA degradation. Furthermore, semi-quantitative analysis of intracellular localization of terminal deoxynucleotidyl transferase-mediated dUTP-biotin nick end labeling TUNEL) showed a significant ($p < 0.001$) increase in the apoptotic index calculated for bronchiolar 73.5%, terminal bronchiolar (65%), and respiratory bronchiolar 60.8% segmental epithelial components as well as alveolar (55%) epithelia. Analysis of immunohistochemical expression of apoptosis-related gene products also supported the hypothesis that benzene can induce apoptosis in chemosensitive target cells in the lung parenchyma. Quantitative immunhistochemistry showed a statistically significant increase $p < 0.001$ in the immunoreactive staining index for cytochrome *c*, Apaf-1 (apoptosis activating factor-1), DNA fragmentation factor, and representative cysteine proteases including caspase-1, caspase-2L, caspase-8 and caspase-9. Thus this is the first study of the respiratory system that demonstrates that benzene inhalation induces lung cell apoptosis as confirmed by DNA electrophoresis, *in situ* nick end labeling, and the upregulation of apoptosis-related gene products that facilitate caspase-cleaved enzymes which lead to cell degradation via programmed cell death. These responses may represent an important defense mechanism within the parenchymal cells of the respiratory system that reduce mutational hazard and the potential carcinogenic effects of benzene-initiated pathogenesis.

Abbreviations: Apaf-1, apoptosis activating factor 1; ISI, immunoreactive staining index; TUNEL, terminal deoxynucleotidyl transferase-mediated dUTP-biotin nick end labeling

Introduction

Benzene, a well-known human carcinogen, is a commonly used industrial chemical that evokes further toxicological concern because of its potential genotoxic risk as a constituent of gasoline and a by-product of combustion and cigarette smoking (Aksoy, 1988; Yardley-Jones et al., 1991; Snyder et al., 1993; Hoffman et al., 1996; Snyder, 2000). In reviewing the literature, however, there are no *in vivo* studies related to the effects of benzene exposure on lung cell apoptosis. Yet animal studies have shown that the lung is a target organ of benzene tumorigenicity, while human subjects exhibit increased risks for adenocarcinoma and squamous cell carcinoma of the lung when occupationally exposed to benzene (Aksoy, 1989; Yin et al., 1989, 1996a, b; Hayes et al., 1996) as well as to cigarette smoke (Darrall et al., 1998).

The present study was undertaken to characterize the effects of benzene exposure on apoptosis in pulmonary tissue and to identify the cell type(s) targeted by benzene-induced apoptosis. Internucleosomal DNA fragmentation of lung tissue taken from animals exposed to benzene via inhalation was assessed by gel electrophoresis to determine the pattern of base piece fragmentation and by cytochemical analysis using terminal deoxynucleotidyl transferase-mediated dUTP-biotin nick end labeling (TUNEL) to detect programmed cell death in immunohistochemically labeled cell types undergoing apoptosis. To further characterize the cellular localization of apoptosis of lung parenchyma in response to benzene-induced cytotoxicity, the upregulation of protein expression was also examined immunohistochemically for several apoptosis-related gene products. These included cytochrome *c*, which is translocated from the mitochondrial membrane to the cytosol during apoptosis (Liu et al., 1996); apoptosis activating factor-1 (Apaf -1), which may mediate apoptosis downstream of the survival protein Bcl-2 and upstream of the apoptosis-inducing caspases (Zou et al., 1997); DNA fragmentation factor (DFF-45), which induces DNA fragmentation after subsequent activation of caspase-3 (Sakahira et al., 1998); caspase-1, which mediates many of the morphological and biochemical features of apoptosis, including structural dismantling of cell bodies and nuclei, fragmentation of genomic DNA, destruction of regulatory proteins, and propagation of other pro-apoptotic molecules (Chang and Yang, 2000; Eldadah and Faden, 2000; Fadeel et al., 2000; Grutter, 2000; Johnson, 2000; Wang and Lenardo, 2000; Coffey et al., 2001); caspase-2L, a cysteine protease of the caspase family that has been shown to play a role in the apoptotic pathway (Li H et al., 1997; Butt et al., 1998; Gorman et al., 1998); caspase-8, which autocatalytically cleaves itself upon recruitment to the death inducing signaling complex (DISC) in an oligomerization-dependent manner (Donepudi et al., 2003) and thus functions in the death receptor induced apoptotic pathway; and caspase-9, which functions as a key component of the apoptotic machinery and acts to destroy specific target proteins critical to cellular longevity, e.g. poly(ADP)-ribose) polymerase (PARP), which is cleaved by caspase-9 into an 85 kDa apoptotic fragment (Casciola-Rosen et al., 1996; Duan et al., 1996).

Methods and materials

Experimental animals

Twenty male Sprague-Dawley (outbred) rats were randomly divided into two groups. The experimental group consisted of 10 animals with a mean body weight of 199 g and the control group of 10 animals with a mean body weight of 188 g. Each group was further divided into three groups, which were housed in polycarbonate cages.

Design of the benzene exposure unit and inhalation procedure

The benzene exposure experiments were carried out within a walk-in, glass-walled, isolation

chamber that contained transparent units. These served as the exposure spaces. Each unit accommodated a large polycarbonate animal cage and was designed with three major features: a benzene saturated vapor injection system, a mixing and ventilation system, and a monitoring device. Pressurized nitrogen vaporized benzene solvent into saturated vapor at a designated constant volume. The saturated benzene vapor was disseminated throughout the chamber and cage by an air stream delivering 10–15 L/min. The benzene concentrations in the exposure chambers were continuously monitored by an instant flame ionization detector (Hydrocarbon Vapor Meter, Thermo Environmental Instruments, Franklin, MA, USA) and routinely verified by gas chromatography (Hewlett Packard GC 5890/Agilent MS 5973, Wilmington, DE, USA). The exhaust air containing circulated benzene was adsorbed by activated charcoal. All animals were maintained according to the ROC National Science Council animal welfare guidelines. Following an initial period of 3 days to allow acclimation to the exposure units, experimental rats were exposed via inhalation to 300 ppm benzene for 23 h each day for 7 consecutive days. The benzene exposure was terminated each day between 13:00 and 14:00. During this time the rats were weighed and examined for physical signs of morbidity. Control rats were placed in identical units but without benzene exposure. All animals were maintained at room temperature with 20% humidity and on a 12 h light cycle.

Tissue processing and immunohistochemistry

At the time of killing, each rat was anesthetized with sodium pentobarbital (25 mg/kg, i.p.) and a thoracotomy was performed whereby a small sample of lung tissue for DNA analysis was removed as described below. Each animal was transcardially perfused with physiological saline followed by perfusion with Zamboni's fixative. Subsequent to fixation, the trachea was cannulated and the lungs were further fixed by intratracheal instillation of cold fixative. The trachea and attached pulmonary lobes were removed *en masse* from the thoracic cavity and postfixed in Zamboni's fixative overnight at 4°C. Following postfixation, the major right and left lobes were removed from the bronchi, dehydrated in graded ethanols, cleared in xylene, and infiltrated. Paraffin blocks were sectioned at 5–7 μm on a rotary microtome and mounted for immunostaining as serial sections on Superfrost/Plus slides Fisher; Taiwan. Sections were deparaffinized in xylene and rehydrated with distilled water, and rinsed in 0.1 mol/L phosphate-buffered saline (PBS), pH 7.2. Endogenous peroxidase expression was blocked by incubation of tissue sections with 0.3% hydrogen peroxide in methanol for 30 min at room temperature. Sections were rinsed in PBS and nonspecific binding was blocked by additional incubation of tissue sections for 10 min at room temperature with normal horse serum (0.1%), diluted in PBS. Excess normal serum was removed and the sections were incubated at 4°C overnight with primary antisera, the types and dilutions of which are given in Table 1. All primary antisera were diluted in 0.1% BSA and 0.01% sodium azide dissolved in PBS. Following incubation, sections were washed in PBS (3 × 5 min) and incubated for 1 h at 4°C with biotinylated secondary immunoglobulins, rinsed in PBS as above, and complexed in a third incubation at 4°C with avidin-biotinylated peroxidase for 1 h. Following PBS washes, the sections were rinsed in acetate buffer for 10 min

Table 1. Primary antibodies, their sources and dilutions

Primary antibody	Type	Dilution	Source
Cytochrome *c*	Rabbit polyclonal	1:100	SCB[a]
Apaf 1	Rabbit polyclonal	1:200	SCB
DNA fragmentation factor	Mouse monoclonal	1:100	NL[b]
Caspase-1	Rabbit polyclonal	1:200	SCB
Caspase-2L	Rabbit polyclonal	1:100	SCB
Caspase-8	Mouse monoclonal	1:100	SCB
Caspase-9	Rabbit polyclonal	1:100	SCB

[a]Santa Cruz Biotechnology, CA, USA.
[b]Novocastra Laboratories Ltd., UK.

and the peroxidase reaction was developed in a 0.03% solution of 3,3′-diaminobenzidine tetrahydrochloride (DAB: Sigma Chemical, St. Louis, MO, USA) in acetate buffer (0.01 mol/L) combined with nickel enhancement (Shu et al., 1985). The specificity for antisera was demonstrated by the lack of stain when diluted primary antisera were preabsorbed with the respective antigens or replaced by normal sera. Slides were counterstained with Van Geison's stain, dehydrated in graded ethanol, and coverslipped. In instances where cellular details of selected epithelial segments required clarification, e.g., neuroendocrine cells, adjacent serial sections were immunohistochemically stained for antigens expressing synaptophysin and/or chromogranin to confirm morphology.

Terminal deoxynucleotidyl transferase-mediated dUTP-biotin nick end labeling (TUNEL)

To assess apoptosis, multiple sections mounted on slides were serially designated for TUNEL reaction, positive control (enzyme treated) and negative control (unreacted TUNEL label only). Treatment of the sections was carried out simultaneously using the reagents provided in the In Situ Cell Death Detection Kit (Roche) and according to instructions of the manufacturer with modifications. In lieu of the commercial peroxidase, anti-peroxidase-conjugated (POD) substrate, 50 µl of a DAB solution modified as described earlier for immunohistochemical staining was applied to each section following TUNEL incubation. Sections were subsequently rinsed in distilled water, counterstained with either Van Geison's stain or methyl green, washed and dehydrated through graded ethanols, and cleared in xylene. Sections were coverslipped and the results were documented using an Olympus M-60 microscope equipped with an Olympus digital camera and/or an Olympus BH2 system with attached 35 mm camera.

Quantitation of apoptotic cells and calculation of apoptotic index

A semi-quantitative procedure was implemented to count the number of cells undergoing apoptosis and thus to calculate an apoptotic index or the percentage of cells within the total parenchymal population of the lung undergoing programmed cell death. The epithelial tissue of four parenchymal components of the lung was subjected to quantitative analysis; this included (i) bronchioles, (ii) terminal bronchioles, (iii) respiratory bronchioles, and (iv) alveoli. For each lobe, seven intervals of serial sections were selected which contained a full face of lung tissue from the beginning to the end of each block. For each section of lung tissue, two fields representative of each parenchymal component were randomly selected and the stage coordinates were recorded to avoid replication and to provide for subsequent recall of images for detailed analysis if warranted. This sampling procedure yielded <56 sampled sites per lung lobe or 14 component fields per lung lobe. Sections were examined under an Olympus BH2 microsocope with the aperture iris diaphragm adjusted to 50% of the objective pupil and condenser numerical aperture closed down to 0.4–0.5 to optimize contrast and depth of focus. Using a $\times 100$ oil-immersion objective and an ocular lens with a 0.25×0.25 mm (1 mm $\times$ 100) graticule grid as reference, counting began at the x coordinate and moved along the y axis until <20 cells were counted per component. The procedure was repeated for a recount of TUNEL-stained cells only. The apoptotic index for each field was calculated as the number of positive TUNEL-stained epithelial cells divided by the total number of epithelial cells counted per field. The mean apoptotic index was calculated as the total number of TUNEL-stained epithelial cells recorded for each parenchymal component divided by the total number of epithelial cells counted per parenchymal component per lobe per animal ($n = 10$). As in the case of apoptosis quantification, the immunocytochemically stained epithelial tissue of the four parenchymal components

of the lung were assessed for the degree of staining for each primary antibody. Unlike the TUNEL procedure, a single site per component was randomly selected from each of the 7 sections sampled as above from the sectioned block. Thus, this procedure yielded <28 sampled sites per component per lung lobe per animal ($n = 10$). Subsequent to the cell counting method as described above for TUNEL, an immunoreactive staining index (ISI) for each field was calculated as the number of positive-stained epithelial cells divided by the total number of epithelial cells counted per field. The mean ISI was calculated as the total number of immunoreactively stained epithelial cells recorded for each parenchymal component divided by the total number of epithelial cells counted per parenchymal component per lobe per animal ($n = 10$).

Detection of DNA fragmentation

At the time of sacrifice, a small portion of lung lobe was ligated with suture in each experimental and control rat subsequent to thoracotomy but preceding vascular perfusion. Approximately 200 mg of lung tissue was removed distal to the ligation. The excised lung tissue sample was immediately frozen and stored in liquid nitrogen. The remaining lung tissue proximal to the ligation was processed for immunohistochemical studies following fixation as described above. DNA was extracted from the excised lung tissue samples according to a modified method of Goelz et al. (1985). Briefly, the frozen lung tissue was minced on ice and subsequently placed in 750 µl of lysis buffer, containing 10 mmol/L Tris-HCl pH 7.8, 5 mmol/L EDTA pH 8.0, 0.5% sodium dodecyl sulfate (SDS), and 0.8 mg/ml proteinase K, and incubated at 55°C for 16 h. DNA samples were extracted, precipitated, washed, and resuspended in TE buffer (10 mmol/L Tris-HCl pH 7.4 and 1 mmol/L EDTA pH 8.0). All DNA samples were treated with DNase-free RNase (Boehringer Mannheim) at 37°C for an hour and then extracted again, precipitated, and resuspended in 50 µl of TE buffer. DNA concentration was determined based on 260 nm absorption using a Beckman DU-600 spectrophotometer. DNA fragmentation among samples was detected using conventional agarose gel electrophoresis. DNA samples were loaded onto 1.2% (w/v) agarose horizontal slab gels and electrophoresis was carried out in 1× TAE buffer (40 mmol/L Tris-acetate and 1 mmol/L EDTA) for 15 min at 50 V followed by 60 min at 80 V. Gels were stained using ethidium bromide and photographed under UV illumination.

Statistical analyses

All statistical analyses were carried out using Graph Pad Prism 4. The significance of differences between the experimental and controls groups for the apoptotic index, immunoreactive staining index, and weight changes was evaluated by Student's *t*-test for unpaired data and all data are expressed as mean + SEM. Additional analysis included a Mann–Whitney nonparametric test of medians.

Results

Weight changes and premortem appearance

As shown in Figure 1, during the week of benzene exposure the experimental rats exhibited an exponential decrease in body weight beginning on the second day of exposure (day 5 of graph). By the end of the exposure period the experimental rats had a mean body weight loss of 26.2 g. Compared to the body weight of age-matched controls, the benzene-exposed rats lost a mean of 40.7 g body weight by day 7 of exposure. No mortality occurred during the experiment.

TUNEL staining and immunocytochemistry

Following the enzymatic *in situ* labeling, microscopic examination revealed stained cells

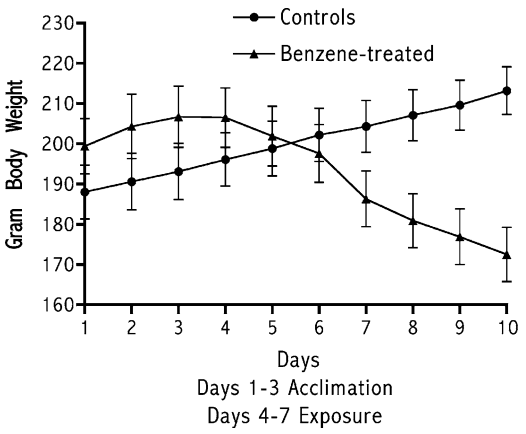

Figure 1. Change in body weight(grams) in benzene-treated rats and age-matched controls. Benzene exposure began on day 4 following three days of acclimation to the exposure chambers.

undergoing apoptosis in all parenchymal components of the lung tissue. In Figures 2 and 3 are shown low- and high-magnification micrographs of TUNEL-stained pulmonary tissues from benzene-treated animals. The cytochemical reaction of TUNEL is shown for bronchiolar epithelium (Figure 2A, B), for a segment of terminal and respiratory bronchiole (Figure 2C) and for alveolar epitheliim (Figure 2D). Condensation of nuclei and some nuclear segmentation can be observed as well as some cell shrinkage. At higher magnification, several morphological features of apoptosis can be observed. In all cells labeled with TUNEL, the nuclei exhibited the hallmark change of intense chromatin condensation, usually with margination (Figure 3A) and with and without distinct fragmentation (Figure 3B). In addition to nuclear changes, reduction in cytoplasmic volume, which is regarded histopathologically as a primary morphological change of apoptotic cells, was clearly noted in numerous pulmonary cells of the experimental tissues. This reduction and its consequence of cell shrinkage often led to an irregular luminal appearance quite striking within the columnar cells of the pseudostratified epithelia of larger bronchioles (Figure 2A, B) where the shrunken cells are recessed from the luminal border (Figure 3A). TUNEL-stained cells frequently exhibited reduction in cytoplasmic volume which at times presented with a perinuclear halo-like appearance or as a vaculolated region within the cytosol (Figures 2A and 3B). Cell membrane changes often accompanied a general change in cytoplasmic configuration due to the apparent loss of lateral adhesive forces of cell junctions that are extremely important in the maintenance of epithelial integrity. Thus, cells were found to have irregular contours along their lateral membranes beyond that normally found in complex pseudostratified columnar epithelia of bronchioles (Figure 3A). The occurrence of membrane blebbing distinct from luminal sloughing was also observed (Figure 3C), which appeared to contribute further to the dissolution of the cell cytoplasm and integrity. Membrane-bound apoptotic bodies were frequently encountered along the basal border of the bronchiolar epithelia or within the lateral contours of the cell membrane (Figure 3D). Apoptotic bodies were also observed in epithelia of terminal and respiratory bronchioles as well as within the alveolar walls. Other observations of histological changes associated with apoptosis included the attenuation and/or loss of ciliated membrane in the bronchiolar and terminal bronchiolar epithelial cells.

Calculation of the apoptotic index from the quantification of TUNEL-stained cells shows a significant increase in epithelial apoptosis. The graph in Figure 4 shows the extent of this increase for each parenchymal component. The epithelia of larger bronchioles exhibited the greatest extent of apoptosis (B, 73.5%), while terminal bronchioles (TB, 65%), respiratory bronchioles (RB, 60.8%), and alveoli (A, 55.6%) all showed an equally significant increase ($p \geq 0.001$) over control tissue, which exhibited negligible apoptosis for all parenchymal components (B 5.09%; TB 4.5%; RB 4.3%; A 3.8%). In addition to the occurrence noted in the epithelial cells, apoptosis appeared significantly increased in stromal cells, although these cells were not quantified. Apoptotic cells were most apparent among macrophages

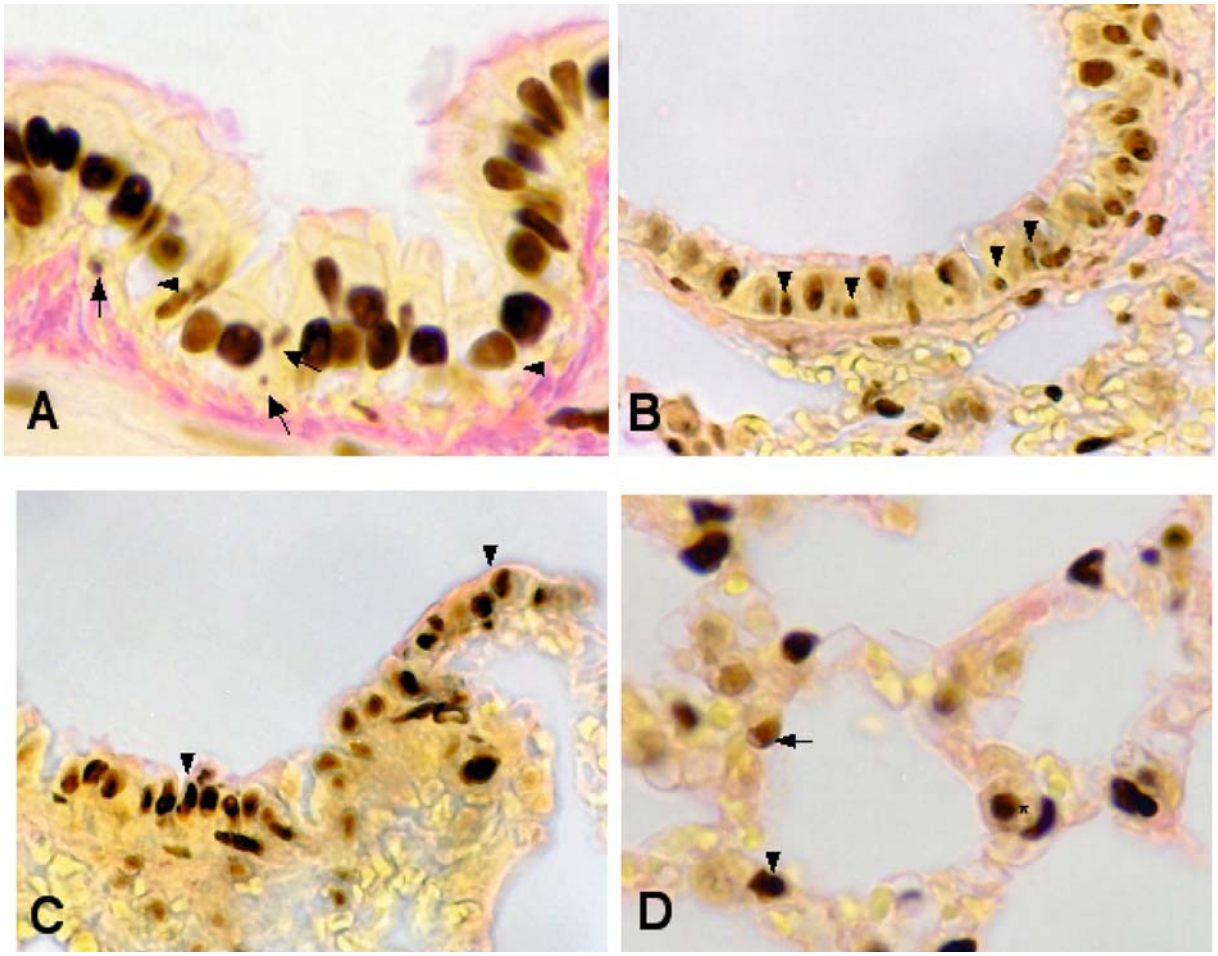

Figure 2. TUNEL-stained lung epithelia from benzene-treated animals. (A) Epithelial cells of a bronchiole showing varying degrees of changes in the darkly stained nuclei. Apoptotic cell bodies can be seen within the basal and lateral compartments of the epithelia (arrowheads), which indicate the terminal events of apoptosis. Clear cytoplasm can be seen in the cells undergoing cellular changes leading to a loss of cytoplasmic volume and shrinkage (arrows; ×20). (B) This low-magnification micrograph of a tangential section of bronchiolar epithelium shows condensed and segmented nuclei (arrowheads) and the irregular appearance of the lumen of the pseudostratified epithelium resulting from cell shrinkage (×20). (C) A segment of columnar cells of a terminal bronchiole (left arrowhead) and its transition to cuboidal cells of respiratory bronchiolar epithelium (right arrowhead) showing condensed nuclei in both segmental components of parenchyma (10). (D) Alveoli with apoptotic cells. Both alveolar type I (arrowhead) and type II (arrow) cells underwent apoptosis with benzene exposure as well as pulmonary macrophages including alveolar macrophages (asterisk) (×10).

within the walls of pulmonary vessels, within the connective tissue underlying the epithelia, and within the walls of the alveoli. The nuclei of smooth-muscle cells lining the vessels and bronchioles also showed increased apoptotic activity.

Electrophoretic analysis of genomic DNA

As shown in Figure 5, the lanes containing DNA isolated from benzene-treated rats exhibit the characteristic ladder pattern consisting of ordered multiples of an approximately 200 bp

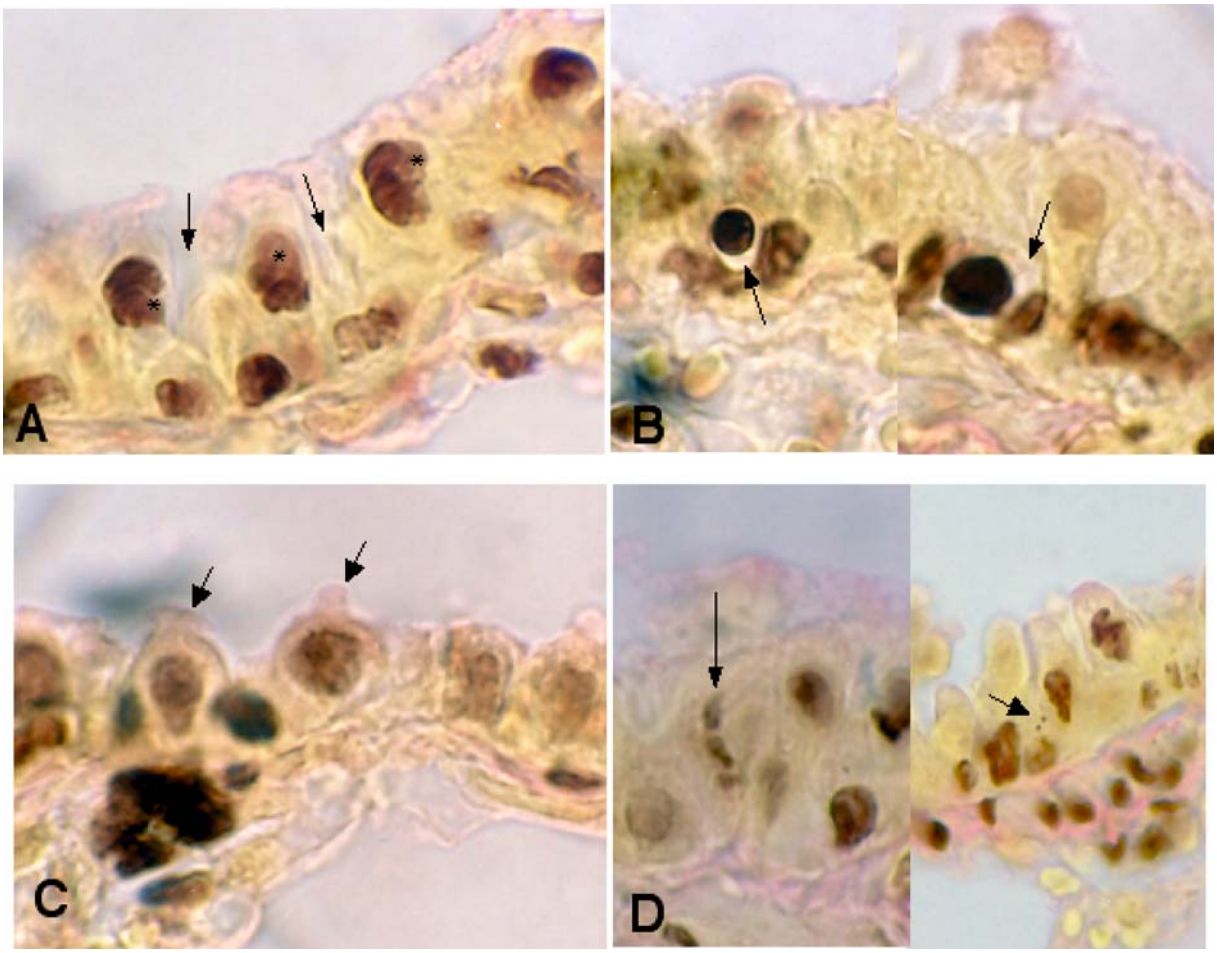

Figure 3. (A) Higher magnification of bronchiolar epithelium shows apoptotic cells with early phases of nuclear segmentation (asterisks). Apoptosis-induced cytoplasmic reduction led to cell shrinkage and changes in the adhesive integrity of the lateral margins (arrows) (×40). (B) A number of cell types were found to undergo apoptosis including ciliated cells, nonciliated cells, basal cells, and, as shown, here a neuroendocrine cell (arrow, left panel) and a Clara cell (arrow, right panel) both with a highly condensed nucleus surrounded by a margin of clear cytoplasm (×40). (C) Blebbing, as shown in this segment of terminal bronchiolar epithelium (arrows) was frequently seen in epithelia undergoing apoptosis (×40). (D) Apoptotic bodies were evident in the pulmonary epithelia of benzene-treated animals. In two sample segments of epithelium, the early formation of apoptotic bodies is shown in the left panel (arrow) and advanced forms in the right panel (arrow) (×20).

internucleosomal subunits, indicative of apoptotic DNA degradation. In contrast, the lane containing control DNA shows no evidence of basepiece fragmentation.

Immunocytochemical changes

Changes in immunoreactivity from the control patterns of constitutive staining accompanied all of the apoptosis-related gene products as assessed by immunocytochemical localization. These are described as follows.

Cytochrome c

A striking difference in cytochrome *c* localization was noted between experimental and control tissues with regard to the disposition of the

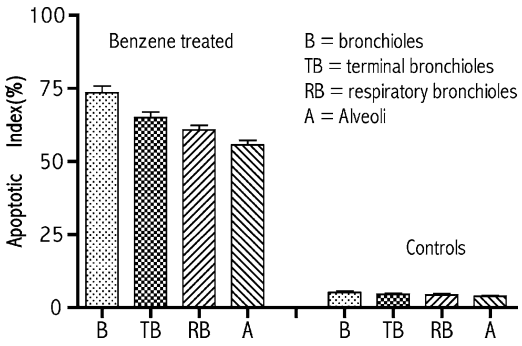

Figure 4. The apoptotic index calculated for each parenchymal component of lung epithelium in benzene-treated animals and controls. A significant increase in apoptosis ($p < 0.001$) was found for all parenchymal components in the benzene-treated rats compared to controls.

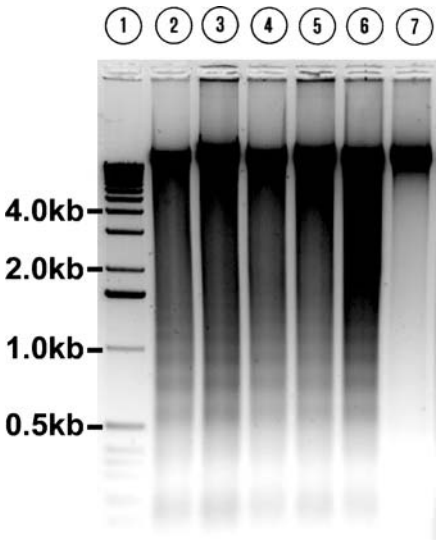

Figure 5. Electrophoretic gels stained with ethidium bromide and showing a standard in lane 1, samples of benzene exposed lung in lanes 2–6, and a normal control sample in lane 7. The lanes containing DNA isolated from benzene-treated rats exhibit the characteristic ladder pattern consisting of ordered multiples of approximately 200 bp subunits indicative of the DNA degradation. In contrast, the lane containing control DNA shows no evidence of basepiece fragmentation.

immunoreactive chromagen and its intensity. The immunocytochemical staining of cytochrome *c* was easily identified by its characteristic punctate appearance, which heavily stained the cytoplasmic component of the cell as shown in Figure 6B. In benzene-treated lung parenchyma, the epithelial cells stained intensely and the stain was widely dispersed throughout the cytoplasm. The dense cytosolic granular staining pattern markedly defined the shape of each cell and its absence clearly indicated the position of the cell nucleus. In contrast, the control parenchymal cells exhibited faint and infrequent immunoreactive staining which showed limited perinuclear and basal localization especially in taller columnar cells of larger bronchioles. As indicated in Figure 3C, significant cytochrome *c* immunoreactive staining was found within all epithelial passageway components as indicated by the mean immunoreactive staining index (ISI) of each, including alveoli (72%), bronchioles (83%), terminal bronchioles (83.9%), and respiratory bronchioles (81%). Stained cells of all parenchymal components from the benzene-treated animals were significantly greater ($p < 0.001$) than in control animals.

Apoptotic protease activating factor Apaf-1

Apaf-1 immunocytochemical staining closely resembled the granular punctate stain of cytochrome *c* and likewise stained the cytoplasmic component, leaving a conspicuous absence of stain over the nuclear region. Although the entire cytosol exhibited heavy staining, a particularly intense staining concentration was frequently observed within the apical portion of the cell, forming a dense supranuclear capping of granules under the luminal boundary. This was commonly seen in both the columnar epithelial cells of bronchioles and terminal bronchioles as well as cuboidal cells of respiratory bronchioles. Figure 7B shows examples of this capping. Apaf-1 immunoreactivity was localized in all cell types within the epithelium. Little immunoreactive staining was observed in control parenchyma. As shown in Figure 7C, the ISI was significantly increased ($p < 0.001$) for all epithelial segments of the pulmonary passageway including alveoli (55.3%), bronchioles

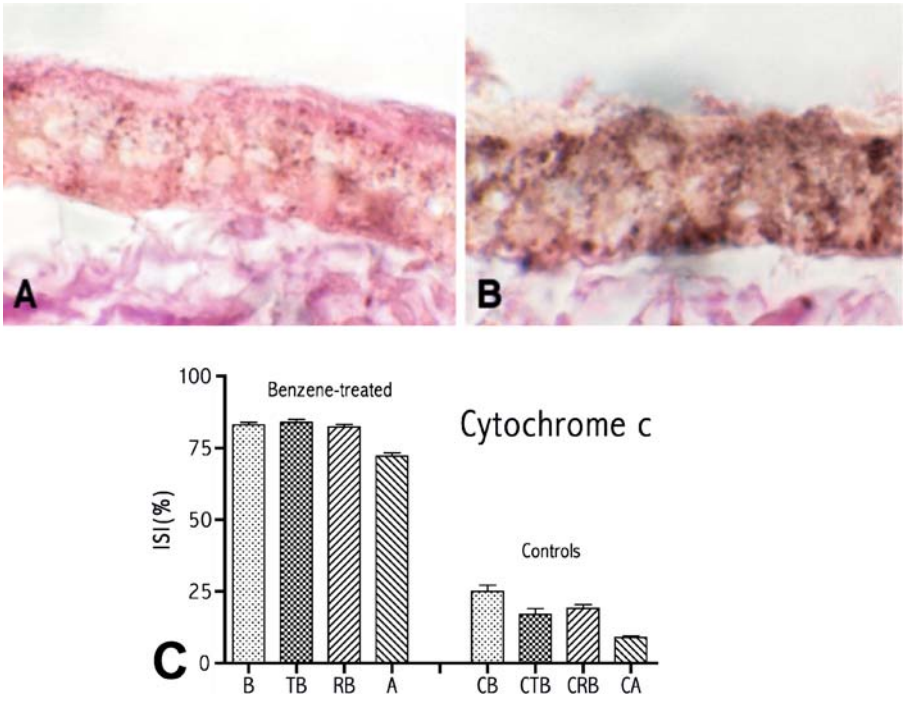

Figure 6. Immunocytochemical staining of cytochrome *c* in a segment of terminal bronchiole from a control rat (A) and a benzene-treated rat (B; ×40). The heavy punctate granules found densely distributed throughout the cell cytoplasm in all epithelial cells of the parenchyma in benzene-treated animals were markedly less patent in control tissues. (C) The immunoreactive staining index (ISI) showed a significant increase ($p < 0.001$) in the cellular expression of cytochrome *c* in benzene-treated animals compared to controls for all parenchymal components of the pulmonary passageway.

(75.4%), terminal bronchioles (72.5%), and respiratory bronchioles (71%).

DNA fragmentation factor

The immunoreactive stain for DNA fragmentation factor was notably expressed in the lung parenchyma of benzene-treated rats as punctate granules within the cytosolic component of epithelial cells, as shown in the example of Figure 8B. As in the case of Apaf-1 immunoreactivity, a dense concentration of granules was noted in the apical portion of epithelial parenchyma. This capping was largely present in both ciliated and nonciliated epithelial cells. A more random distribution of granules was exhibited throughout the cytoplasm of basal cells, in bronchiolar Clara cells, and in neuroendocrine cells. In control tissues, epithelial cells exhibited little staining. As shown in Figure 8C, a significant increase in immunocytochemical expression ($p < 0.001$) was found within all parenchymal components of the pulmonary passageway including alveoli (46.6%), bronchioles (75.7%), terminal bronchioles (76%), and respiratory bronchioles (73.1%) compared to immunoreactively stained cells of control tissues.

Interleukin-1b converting enzyme, ICE (caspase-1)

Immunoreactive staining for caspase-1 exhibited a marked granular punctate pattern found predominantly in the cytoplasm and occasionally in the nuclei of the parenchyma. The dense staining, represented by both small and large

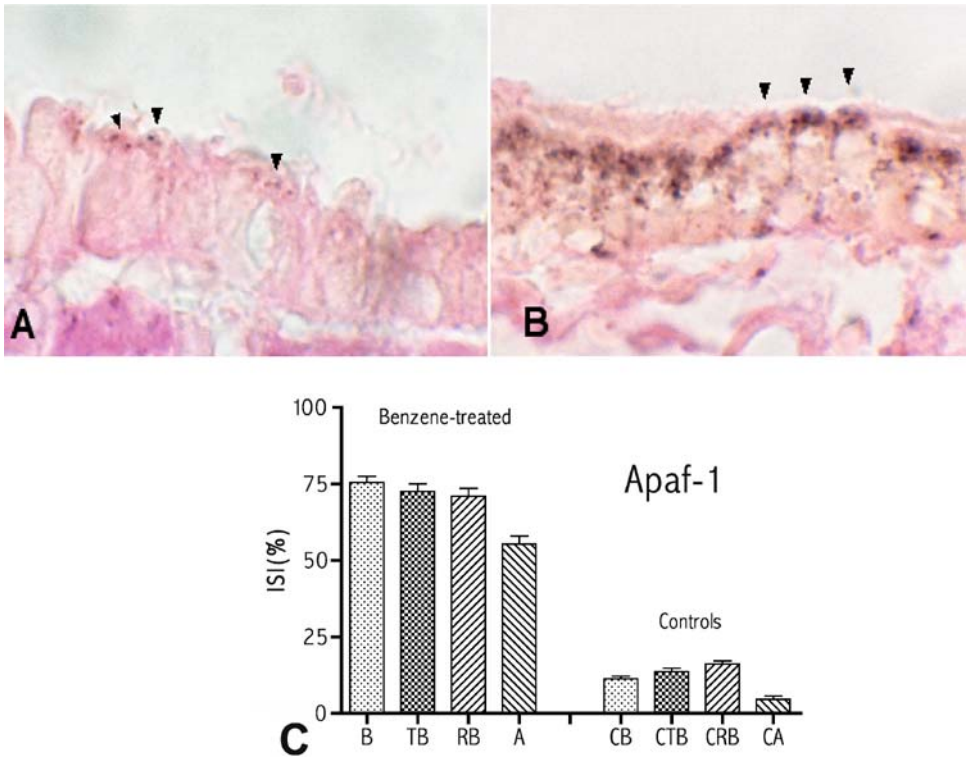

Figure 7. Immunocytochemical staining of Apaf-1 in a segment of terminal bronchiolar epithelium from a control rat (A) and a benzene-treated rat (B; ×40). A particularly intense staining could be noted in the apical portion (arrowheads) of immunoreactive cells. In contrast, the control tissues exhibited significantly less staining. As indicated in the ISI graph (C), a significant increase ($p < 0.001$) was found in the cellular expression of Apaf-1 for all parenchymal components of the pulmonary passageway from benzene-treated animals.

granules as shown in Figure 9B, appeared widely dispersed throughout the cells and was present within the various epithelial cell types of the lung parenchyma. Alveolar immunoreactive staining tended to appear more diffuse within the cell, while more commonly a punctate granular stain was characteristic of bronchiolar, terminal, and respiratory bronchiolar epithelia with frequent apical capping. Although quantitatively less in control epithelia, caspase-1-immunoreactive cells were occasionally localized in control lung parenchyma but were largely limited to bronchiolar cells and especially within the apical region of the epithelia (Figure 9A) and in newly sloughed cells. As shown in Figure 9C, a significant difference ($p < 0.001$) was found in the ISI for all epithelial segments of the pulmonary passageway including alveoli (42.1%), bronchioles (62.6%), terminal bronchioles (56.9%), and respiratory bronchioles (56.6%) compared to immunoreactively stained cells of control tissues.

Caspase-2L

Unlike the case of previously noted apoptosis-related gene products, caspase-2L immunoreactivity was characterized by a diffuse cytoplasmically granular staining pattern, the intensity and density of which appeared comparatively less marked as shown in the example of Figure 10B. The small granules of the chromagen yielded a pepperlike stain that was faint but consistent.

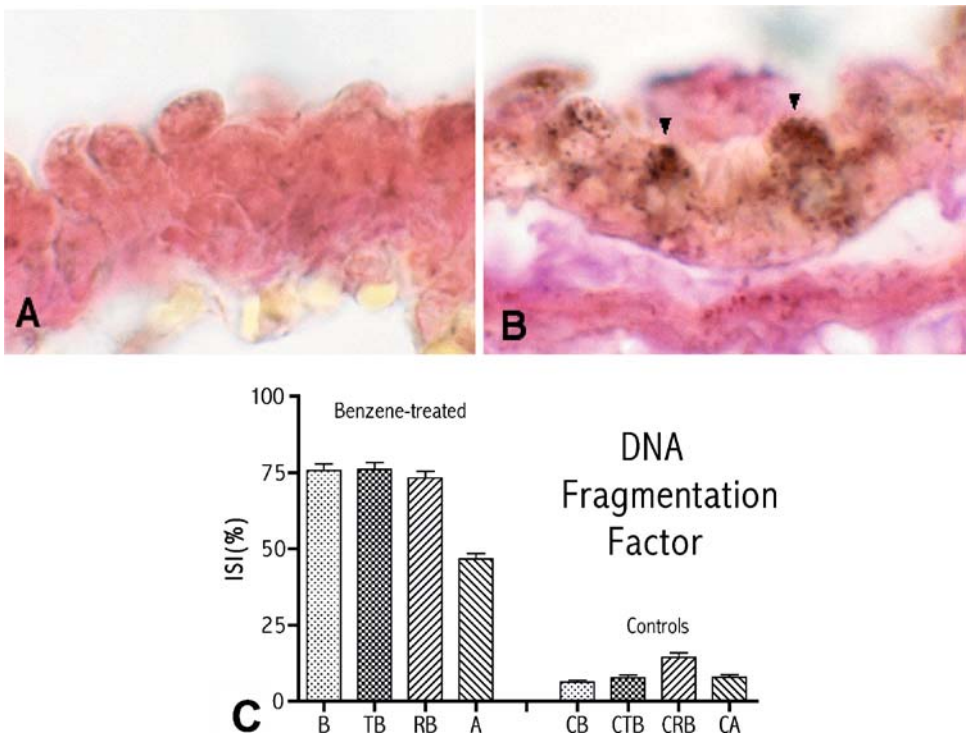

Figure 8. Immunocytochemical staining of DNA fragmentation factor in a segment of bronchiolar epithelium from a control rat (A) and a terminal bronchiole from a benzene-treated rat (B; ×40). The punctate granular stain was heavily dispersed within the cytosolic component of the epithelial cells and often found to aggregate in the apical portion of epithelial cells from experimental tissues (arrowheads). Only negligible staining was found in control tissues. As indicated in the ISI graph (C), a significant increase ($p < 0.001$) was found in the cellular expression of this apoptosis-related protein for all parenchymal components of the pulmonary epithelium in benzene-treated animals.

Cells of control tissues exhibited only negligible staining. As indicated in Figure 10C, all epithelial cell types in benzene-treated lung tissues exhibited some degree of caspase-2L immunoreactive staining and all parenchymal components of epithelia showed a significant increase ($p < 0.001$) in the immunoreactive staining index including alveoli (41.8%), bronchioles (71.1%), terminal bronchioles (67.3%), and respiratory bronchioles (64.4%) compared to control tissues.

Caspase-8

In contrast to immunoreactive staining patterns of previous apoptosis-related gene products, caspase-8 staining was limited exclusively to the nucleus. Thus, the concentrated heavy granular and punctate stain was found to easily demarcate epithelial cells undergoing initial apoptotic change. The characteristic caspase-8-stained nuclei can be seen in the cells of Figure 11B. All epithelial cell types of benzene-treated lung were subject to caspase-8 labeling, while little staining was evident in the epithelia of control tissues (Figure 11A). As shown in Figure 11C, a significant increase caspase-8 immunoreactive staining was found in alveolar (43.3%), bronchiolar (62.8%), terminal bronchiolar (47.9%), and respiratory bronchiolar (58.1%) parenchymal components of benzene-treated animals.

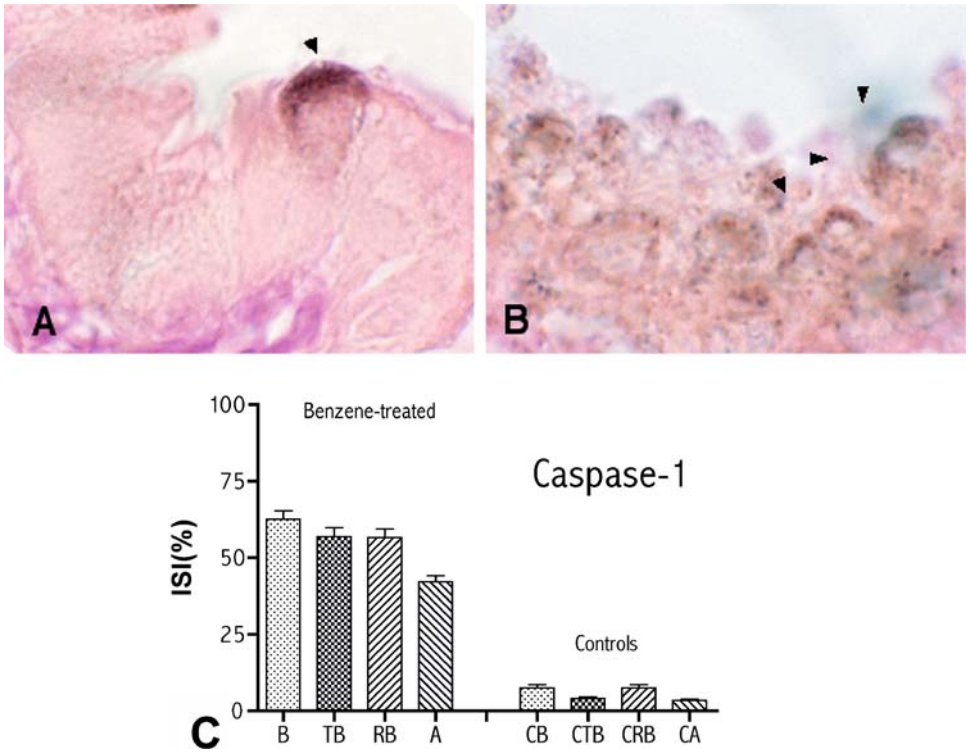

Figure 9. Immunocytochemical staining of caspase-1 in the bronchiolar epithelium from a control rat (A) and an experimental rat (B; ×40). Although the punctate granular stain was distributed within the cytoplasm, capping was frequently noted in stained cells from the benzene-treated rat (arrowheads). This pattern was also found in control tissues when staining was present. As indicated by the ISI graph (C), a significant increase ($p < 0.001$) was found in the cellular expression of caspase-1 in the epithelia of all parenchymal components from benzene-treated animals compared to controls.

Caspase-9

The pulmonary epithelial cells of the benzene-treated animals all exhibited immunoreactive staining for the apoptosis-related gene product, caspase-9. The characteristic staining was a light granular stain that was largely limited to the cytoplasmic component of cells in bronchioles, terminal bronchioles, and respiratory bronchioles, and which at times formed darker aggregates or clumps within the cytosol. Unlike the bronchiolar pattern of staining, caspase-9 consistently stained the nuclei of alveolar pneumocytes presumably undergoing apoptotic changes, as shown in the example of Figure 12B. Negligible staining was present in the bronchioles of control animals, where the target cells appeared to be limited to occasional cells within the epithelia and those epically positioned cells undergoing sloughing. Immunoreactive label in the epithelia of experimentally treated animals appeared to favor ciliated cells and basal cells, whereas Clara cells were often devoid of immunoreactive stain. Quantification of the immunoreactive stain (Figure 12C) for epithelial cells from the experimental lung tissues showed a significant increase in staining ($p < 0.001$) compared to control tissues including those found in alveoli (48.8%), bronchioles (69.1%), terminal bronchioles (66.1%), and respiratory bronchioles (65.1%).

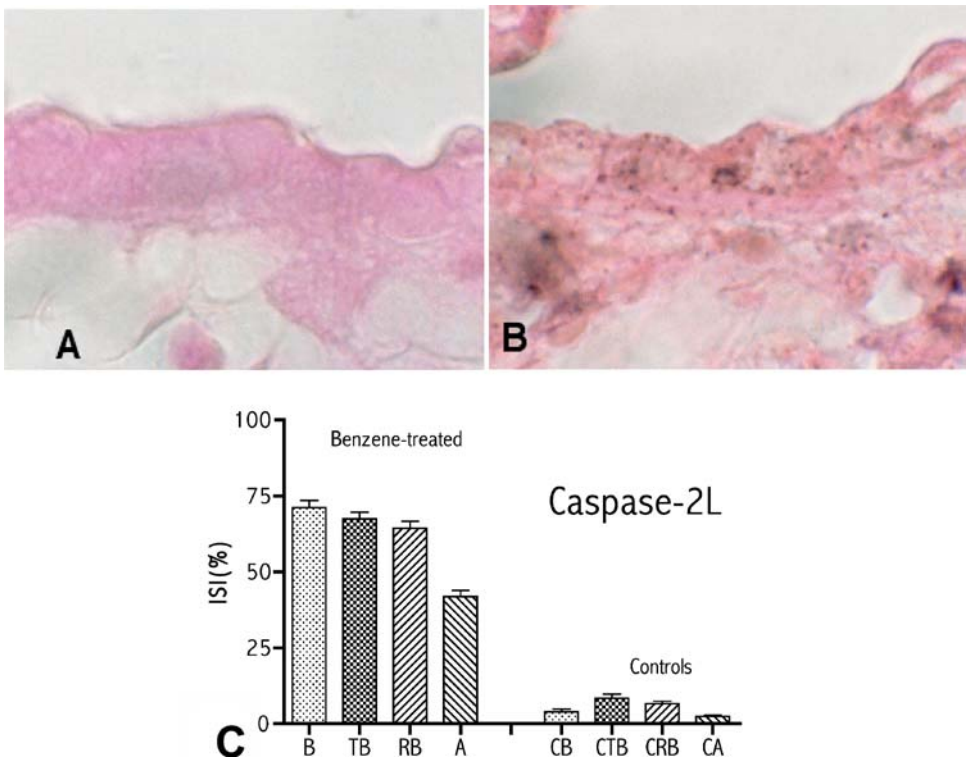

Figure 10. Immunocytochemical staining of caspase-2L in a segment of a respiratory bronchiole from a control rat (A) and a benzene-treated rat (B; ×20). Although less dense in distribution, the stained granules yielded a pepperlike pattern still easily defined by its cytoplasmic localization in the benzene-treated animals. The capping pattern of staining was not observed in immunoreactive cells. Negligible staining was found in all control tissues. As indicated in the ISI graph (C), a significant increase ($p < 0.001$) was found in the cellular expression of caspase-2L in benzene-treated animals compared to controls for all parenchymal components of the pulmonary passageway.

Discussion

From the evidence provided above, benzene exposure induced apoptotic changes in the parenchymal components of the lung that significantly exceeded the events of programmed cell death in normal control tissues. As demonstrated by the gel electrophoresis of the genomic DNA from both animal groups, only the samples from the benzene-treated rats exhibited the characteristic 180–200 bp internucleosomal fragments that form subsequent to the initial cleavage into 300 kb and 50 kb (Brown et al., 1993) and the multiples of which form the characteristic DNA "ladder" pattern upon electrophoresis (Wyllie, 1987). In addition to the evidence for the loss of DNA integrity, the gel ladder appeared related to the changes in nuclear morphology supported in the present study by the statistically significant apoptotic index (Figure 1C). Since cells lining the respiratory tract extending from the bronchiolar segment of the tracheobronchial region generationally through the alveoli were found to exhibit various degrees of nuclear fragmentation, this may indicate that parenchymal cells may respond differentially to the exposure time and duration and thus reflect the heterogeneity observed in the nuclear segmentation of targeted cells undergoing apoptosis.

The segmental component analysis of lung parenchyma used in the present study also indicated that apoptosis was not uniform within

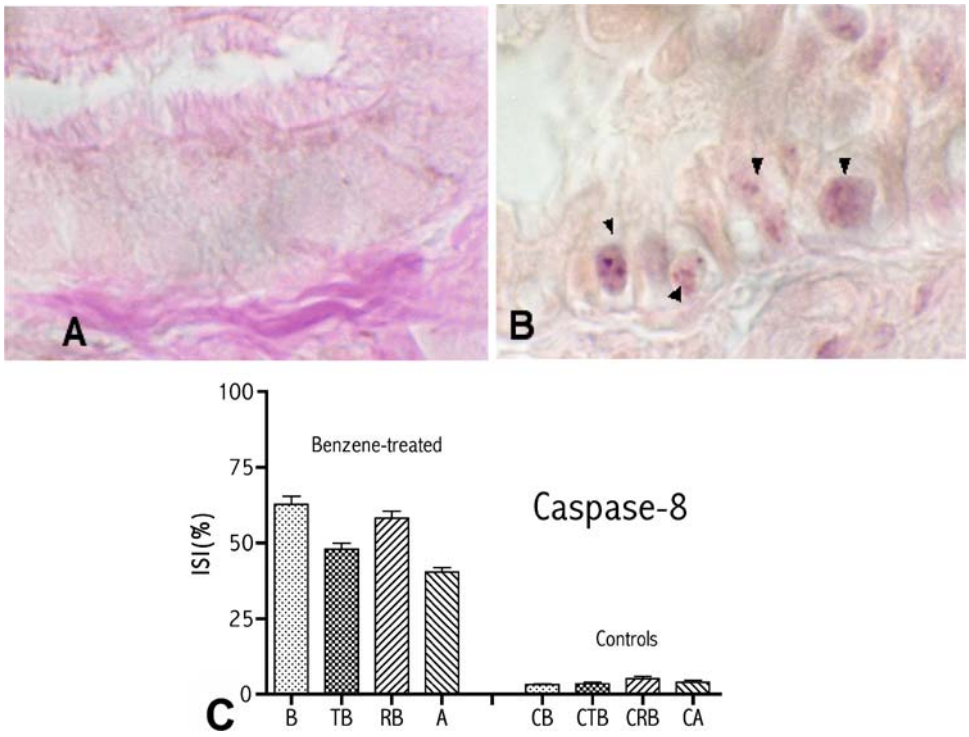

Figure 11. Immunocytochemical staining of caspase-8 in the bronchiolar epithelium of a control rat (A) and a benzene-treated rat (B; ×40). The immunoreactive staining, which was localized exclusively within the nuclei (arrowheads), was found to exhibit a characteristic dense staining pattern that easily demarcated nuclei in the benzene-treated animals. Only negligible staining was found in control tissues. The ISI graph (C) shows a significant increase ($p < 0.001$) in the cellular expression of caspase-8 in benzene-treated animals for all parenchymal components of the pulmonary corridor.

the pulmonary passageways. The data indicate that larger bronchioles were subject to a greater degree of apoptosis (73.5%) compared to the distal segments of the terminal (65%) and respiratory (60.8%) bronchiolar segmental components and alveoli (55.6%). This may indicate that several cell populations that are more prominent within the larger bronchioles (i.e., mucous, ciliated cells) may be more sensitive to the effects of benzene than those found within the terminal and respiratory segments of the bronchioles (i.e., Clara cells, basal cells) or alveoli (pneumocytes I and II), the latter of which exhibited the least degree of apoptosis. Although fewer data are available for aerosolized transport within the respiratory tract compared to the absorption and transport of inhaled reactive and nonreactive gases, it is reasonable to assume a similar absorption concentration gradient may be produced along the liquid lining interface of the upper viscoelastic mucous-rich epiphyses and underlying watery ciliated hypo phase forming the luminal surface of the bronchiolar passageway, which could serially diminish the damaging effects of aerosol-borne molecules. Thus the upper respiratory segmental parenchyma may sustain more acute damage owing to benzene's high solubility in aqueous media and its rapid hydrolysis. Furthermore, the present results indicative of increased apoptotic activity in the epithelia of the terminal and respiratory bronchioles compared to alveoli are not unexpected. This centriacinar region forming a

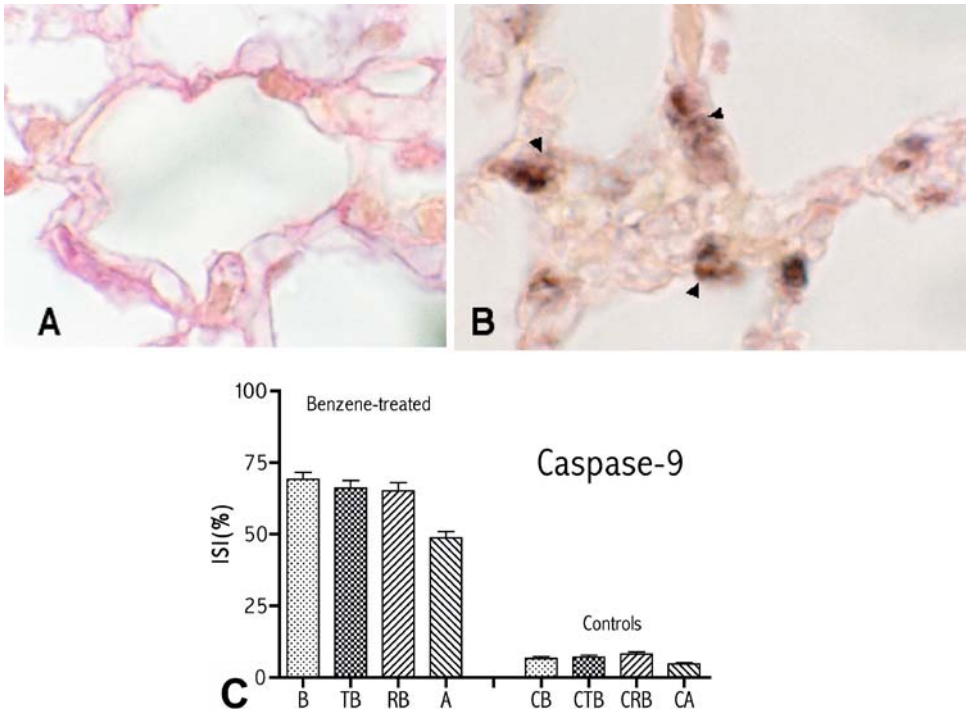

Figure 12. Immunocytochemical staining of caspase-9 in the alveolar epithelium of a control rat (A) and a benzene-treated rat (B; ×40). The immunoreactive stain in alveoli was found to be largely nuclear in distribution (arrowheads) within the tissues from benzene-treated animals. Only negligible staining was found in controls. As indicated in the ISI graph (C), a significant increase ($p < 0.001$) was found in the cellular expression of caspase-9 in benzene-treated animals for all parenchymal epithelia of the pulmonary passageway.

junction between the nonalveolarized conducting terminal bronchioles and the alveolarized respiratory bronchioles has been identified as a primary site for lung injury (St. George et al., 1993; Yeh and Harkema, 1993) arising from a variety of inhaled toxicants ranging from diesel exhaust (Plopper et al., 1973, 1983) and oxidant air pollutants (Plopper et al., 1973; Stephens et al., 1974) to asbestos fibers (Pinkerton et al., 1986). Although a significant variation exists in the histoarchitectural organization of the centriacinar region as well as its cell density and variation in cell type (St. George et al., 1993), its histopathological changes arising from inhalation toxicity, as is the case for the entire respiratory tract, requires a substantial understanding of the processes relevant to convection, molecular diffusion, turbulence, and the dynamic changes in gaseous species, as well as the factors regulating the absorption of inhaled aerosolized molecules.

Supporting data derived from the immunohistochemical analysis of apoptosis-related gene products also support the thesis that benzene can induce apoptosis in chemosensitive target cells in the lung parenchyma. The present results showed that selected gene-products assessed immunohistochemically were all significantly upregulated in the lung parenchyma of benzene-treated animals. The upregulation of caspase-8 and DNA fragmentation factor indicates that benzene-induced apoptosis may be mediated by death receptor activation. Subsequent to the ligand stimulation of receptors in the tumor necrosis factor superfamily (TNRF), the death domain (DED) interactions mediate the specific association of caspase-8(or -10) precursors with these

receptors by way of various classes of adaptors which include TNFR-associated death domain (TRADD), Fas-activated death domain protein (FADD), and Flice-associated huge protein (FLASH) (Porter, 1999). With the stimulation of Fas receptor, the translocation and recruitment of FADD together with a complex of pro-caspase 8 and FLASH to the cytoplasmic tail of Fas is initiated (Imai et al., 1999; Porter, 1999). Thus, the proteolytically activated caspase-8, deprived of its DED-containing receptor anchor (Ashkenazi and Dixit, 1998), translocates from the cytoplasmic tail to the cytoplasm, where it initiates its proteolytic death cascade of downstream caspases, e.g., caspase-3 (Cryns and Yuan, 1998; Porter, 1999), that function as executioner caspases leading to the cleavage of specific intracellular targets. Activation of caspase-3 is also implied by the upregulation of DNA fragmentation factor in the lung parenchymal components of benzene-treated animals. DNA fragmentation, factor as noted earlier, induces DNA fragmentation subsequent to activation by caspase-3, which cleaves the 45 kDa subunit at two sites whereby an active factor is generated to effect the cleavage of chromatin into oligomers of DNA, which also further supports the electrophoretic gel results discussed earlier. It should be noted here that caspase-8 is generally expected to have a cytoplasmic localization since it is essentially activated by binding with the internal part of the membrane FADD/FAS complex as described above. However, in recent studies, caspase-8 has also been shown to localize in the nucleus (Xerri et al., 2000), where it may function in the cleavage of transcription factors since caspase activation can take place by dimerization equally well in the cytoplasm or in the nucleus (Martins et al., 1997). The significance of its nuclear localization in the present study remains unknown but may implicate a benzene-related factor in the biochemical cascade of caspase activation and its subsequent cellular localization.

Caspase-9 was also found to have an upregulated expression in benzene-treated animals and this provides evidence that in addition to death receptor-mediated apoptosis the amplification of apoptosis was induced via mitochondrial damage. The participation of mitochondria has been increasingly accepted as a major pathway for caspase activation (Green and Reed, 1998) and results from the release of cytochrome *c* from the intermembranous space. Subsequent to its entry into the cytosol, the cytochrome *c* binds to the Apaf-1 and ATP, which serves to bind Apaf-1 to pro-caspase-9 and to effect its cleavage to an activated form of caspase-9, which in turn is postulated to proteolytically activate downstream caspases (e.g. caspase-3, -7) leading to apoptosis (Li P et al., 1997). Not only was caspase-9 immunoreactivity found to be significantly increased in all segmental components of the pulmonary passageway of benzene-treated animals, but Apaf-1 and cytochrome *c* were comparably increased in immunoreactive expression as well in all segmental components of the passageway. The staining of cytochrome *c* exhibited a markedly dense and intense chromagen in the experimental tissues, which greatly contrasted with the weak and infrequent staining pattern found in control parenchyma. Thus the cytochrome *c* staining in the experimental tissues provided cellular evidence for the widespread release and distribution of cytochrome *c*, which has been amply demonstrated in the programmed cell changes of cells undergoing apoptosis and which is not a factor in necrosis. The almost identical staining pattern held true for Apaf-1 as well in experimental tissues where the cytosolic distribution of punctate-stained granules exhibited both marked density and pronounced chromagenic intensity. Since caspase-9 was found to have increased expression, it is not surprising to find a concomitant increase in Apaf-1, since it must bind pro-caspase 9 to engage the subsequent activation of pro-caspase-9 to caspase-9. The absence of Apaf-1 immunoreactive staining in the parenchymal cells of control tissues may indicate that this caspase pathway is not normally invoked in the metabolic activation accompanying cell turnover.

In addition to the terminal caspases-8 and -9, caspases-1 and -2L were also assessed in the present study. Overexpression of caspase-2L (ICH/NEDD 2), a member of the ICE family, and one form of mRNA species derived from alternate splicing has been shown to induce programmed cell death that is suppressed by the overexpression of bcl-2. Recent studies have demonstrated that the first cleavage of caspase-2L is accomplished by a caspase-3-like activity (Li H et al., 1997). Immunoreactive positive staining for caspase 2-L in the experimental tissues and its absence in control tissues of the present study would indicate further the role of this caspase in benzene-induced cellular damage. Furthermore, the role of caspase-3 is indirectly supported by the assumption that the initial caspase-2L cleavage was elicited by caspase-3 activity. Although data from knockout mice imply that caspase-1 plays no role in apoptosis, it has recently been shown that chronic caspase-1 activation concomitantly coupled with activation of the executioner caspase-3 may be operative in neuronal cell death (Pasinelli et al., 2000).

Although it was not investigated in the present study, it should be noted that these apoptotic changes could have resulted from the interaction of the pulmonary cellular substrate with benzene metabolite(s). As in the case of other chemical carcinogens, benzene and its metabolites, which most likely mediate the toxicity and mutagenicity of the parent chemical, have been shown to induce apoptosis, which may function to reduce the mutational hazard via the loss of mutated cells. The myelotoxic potential of the phenolic metabolites of benzene, namely, phenol, catechol, hydroquinone, and 1,2,4-benzenetriol, has been assessed in human bone marrow progenitor cells (Moran et al., 1996). The results showed that all the selected metabolites except for phenol induced both marked time- and concentration-dependent apoptosis in HL60 and $CD34^+$ cells. Thus the investigators concluded that benzene metabolites may contribute to benzene myelotoxicity via their ability to induce apoptosis in the progenitor cells. Furthermore, it has been shown that the benzene metabolites 1,4-benzoquinone and 1,4-hydroquinone both induce DNA damage in HL60 cells via intracellular generation of H_2O_2 prior to internucleosomal DNA fragmentation leading to apoptosis (Hiraku and Kawanishi, 1996). These workers also concluded that the elected pathway to apoptosis or mutation may depend on the intensity of DNA damage and the ability to repair DNA. A putative benzene metabolite, 2,3,5-(trisglutathion-S-yl) hydroquinone (TGHQ) has been shown in HL-60 cells to deplete intracellular glutathione (GSH) in a reactive oxygen species (ROS)-independent manner prior to the onset of apoptosis (Bratton et al., 2000). The authors concluded that TGHQ, and possibly other quinol-based toxicants and chemotherapeutics, may induce apoptosis in hematopoietic cells by the depletion of GSH and the subsequent pro-apoptotic ceramide-signaling pathway. Related studies have shown that 1,3-dinitrobenzene increases both the incidence and severity of apoptosis in rat testes (Strandgaard and Miller, 1998), while other studies have shown that benzene also induces an increased rate of apoptosis in peripheral lymphocytes of humans exposed to benzene-contaminated water (Vojdani et al., 1997).

In summary, this is the first study of the respiratory system which demonstrates that benzene-induced apoptosis is accompanied by programmed cell death changes based on the endonucleolytic degradation of genomic DNA as well as the upregulation of apoptosis-related gene products that facilitate caspase-cleaved enzymes that orchestrate cell degradation. Taken together, the events leading up to and including apoptosis may represent the first line of defense to reduce mutational hazard and the potential carcinogenic effects of benzene within the parenchymal cells of the respiratory system.

References

Aksoy M. CRC benzene carcinogenicity. Boca Raton: CRC Press; 1988.

Aksoy M. Hematotoxicity and carcinogenicity of benzene. Environ Health Perspect. 1989;82:193–7.

Ashkenazi A, Dixit V. Death receptors: signaling and modulation. Science. 1998;281:1305–8.

Bratton SB, Lau SS, Monks TJ. The putative benzene metabolite 2,3,5-tris(glutathion-S-yl) hydroquinone depletes glutathione, stimulates sphingomyelin turnover, and induces apoptosis in HL-60 cells. Chem Res Toxicol. 2000;13:550–6.

Brown D, Sun X-M, Cohen G. Dexamethosone-induced apoptosis involves cleavage of DNA to large fragments prior to internucleosomal fragmentation. J Biol Chem. 1993;268:3037–9.

Butt A, Harvey N, Parasivam G, Kumar S. Dimerization and autoprocessing of the Nedd2 (caspase-2) precursor requires both the prodomain and the carboxyl-terminal regions. J Biol Chem. 1998;273:6763–8.

Casciola-Rosen L, Nicholson D, Chong T, Rowan K, Thornberry N, Miller D, Rosen A. Apopain/CPP32 cleaves proteins that are essential for cellular repair: a fundamental principle of apoptotic death. J Exp Med. 1996;183:1957–64.

Chang H, Yang X. Proteases for cell suicide: functions and regulation of caspases. Microbiol Mol Biol Rev. 2000;64:821–46.

Coffey R, Watson R, Fitzpatrick JM. Signaling for the caspases: their role in prostate cell apoptosis. J Urol. 2001;165:5–14.

Cryns V, Yuan J. Proteases to die for. Genes Dev. 1998;12:1551–70.

Darrall K, Figgins J, Brown R, Phillips G. Determination of benzene and associated volatile compounds in mainstream cigarette smoke. Analyst. 1998;123:1095-101.

Donepudi M, Sweeney A, Briand C, Grutter M. Insights into the regulatory mechanism for caspase-8 activation. Mol Cell. 2003;11:543–9.

Duan H, Orth K, Chinnaiyan A, et al. ICE-LAP6, a novel member of the ICE/Ced-3 gene family, is activated by the cytotoxic T cell protease granzyme B. J Biol Chem. 1996;271:16720–4.

Eldadah B, Faden A. Caspase pathways, neuronal apoptosis, and CNS injury. J Neurotrauma. 2000;17:811–29.

Fadeel B, Orrenius S, Zhivotovsky B. The most unkindest cut of all: on the multiple roles of mammalian caspases. Leukemia. 2000;14:1514–25.

Goelz, S, Hamilton, S, Vogelstein, B. Purification of DNA from formaldehyde fixed and paraffin embedded human tissue. Biochem Biophys Res Commun. 1985;130:118–26.

Gorman A, Orrenius S, Ceccatelli S. Apoptosis in neuronal cells: role of caspases. Neuroreport. 1998;9: R49–55.

Green D, Reed J. Mitochondria and apoptosis. Science. 1998;281:1309–12.

Grutter MG. Caspases: key players in programmed cell death. Curr Opin Struct Biol. 2000;10:649–55.

Hayes R, Yin S, Dosemeci M, et al. Mortality among benzene-exposed workers in China. Environ Health Perspect. 1996;104:1349–52.

Hiraku Y, Kawanishi S, Oxidative DNA damage and apoptosis induced by benzene metabolites. Cancer Res 1996;56:5172–8.

Hoffman D, Melikian A, Wynder E. Scientific challenges in environmental carcinogenesis. Prev Med. 1996;25:14–22.

Imai Y, Kimura T, Murakami A, Yajima N, Sakamaki K, Yonehara S. The CED-4-homologous protein FLASH is involved in Fas-mediated activation of caspase-8 during apoptosis. Nature. 1999;398:777–85.

Johnson D. Noncaspase proteases in apoptosis. Leukemia. 2000;14:1695–703.

Li H, Bergeron L, Cryns V, et al. Activation of caspase-2 in apoptosis. J Biol Chem. 1997;272:21010–7.

Li P, Nijhawan D, Budihardjo I, et al. Cytochrome *c* and dATP-dependent formation of Apaf-1/caspase-9 complex initiates an apoptotoic protease cascade. Cell. 1997;91:479–89.

Liu X, Kim C, Yang J, Jemmerson R, Wang X. Induction of apoptotic program in cell-free extracts: requirement for dATP and cytochrome *c*. Cell. 1996;86:147–57.

Martins L, Mesner P, Kottke T, et al. Comparison of caspase activation and subcellar localization in HL-60 and K562 cells undergoing etoposide-induced apoptosis. Blood. 1997;90:4283–96.

Moran JL, Siegel D, Sun XM, Ross D. Induction of apoptosis by benzene metabolites in HL60 and $CD34^{+}$ human bone marrow progenitor cells. Mol Pharmacol 1996;50:610–5.

Pasinelli P, Houseweart M, Brown R Jr, Cleveland D. Caspase-1 and -3 are sequentially activated in motor neuron death in Cu, Zn superoxide dismutase-mediated familial amyotrophic lateral sclerosis. Proc Natl Acad Sci USA. 2000;97:13901–16.

Pinkerton K, Plopper C., Mercer R., et al. Airway branching patterns influence asbestos fiber location and the extent of tissue injury in the pulmonary parenchyma. Lab Invest. 1986;55:688–95.

Plopper C, Dungworth D, Tyler W. Pulmonary lesions in rats exposed to ozone. A correlated light and electron microscopic study. Am J Pathol. 1973;71:375–86.

Plopper C, Hyde D, Weir, A. Centriacinar alteration in lungs of cats chronically exposed to diesel exhaust. Lab Invest. 1983;49:391–9.

Porter AG. Protein translocation in apoptosis. Trends Cell Biol. 1999;10:394–401.

Sakahira H, Enari M, Ohsawa Y, Uchiyama Y, Nagata S. A caspase-activated DNase that degrades DNA during apoptosis, and its inhibitor ICAD. Nature. 1998;391:43–50.

Shu S, Ju F, Fan L. The glucose oxidase-DAB-nickel method in peroxidase histochemistry of the nervous system. Neurosci Lett. 1985;85:169–71.

Snyder R. Overview of the toxicology of benzene. J Toxicol Environ Health. 2000;61:339–46.

Snyder R, Witz G, Goldstein BD. The toxicology of benzene. Environ Health Perspect. 1993;100:293–306.

Stephens R, Sloan M, Evans M, Freeman G. Early response of lung to low levels of ozone. Am J Pathol. 1974;74:31–58.

St. George J, Harkema J, Hyde D, Plopper C. Cell populations and structure/function relationships of cells in the airways. In: Gardiner D, ed. Toxicology of the lung. New York: Raven Press; 1993:81–110.

Strandgaard C, Miller MG. Germ cell apoptosis in rat testis after administration of 1,3-dinitrobenzene. Reprod Toxicol. 1998;12:97–103.

Vojdani A, Mordechai E, Brautbar N. Abnormal apoptosis and cell cycle progression in humans exposed to methyl tertiary-butyl ether and benzene contaminating water. Hum Exp Toxicol. 1997;16:485–94.

Wang J, Lenardo MJ. Roles of caspases in apoptosis, development, and cytokine maturation revealed by homozygous gene deficiencies. J Cell Sci. 2000;113:753–7.

Wyllie A. Apoptosis: cell death in tissue regulation. J Pathol. 1987;153:313–6.

Xerri L, Palmerini F, Devilard E, et al. Frequent nuclear localization of ICAD and cytoplasmic co-expression of caspase-8 and caspase-3 in human lymphomas. J Pathol. 2000;192:194–202.

Yardley-Jones A, Anderson D, Parke D. The toxicity of benzene and its metabolism and molecular pathology in human risk assessment. Br J Ind Med. 1991;48:437–44.

Yeh, H-C, Harkema, J. Gross morphometry of airways. In: Gardiner D, ed. Toxicology of the lung. New York: Raven Press; 1993:55–79.

Yin S, Li G, Tain F, et al. A retrospective cohort study of leukemia and other cancers in benzene workers. Environ Health Perspect. 1989;82:207–13.

Yin S, Hayes R, Linet M, et al. An expanded cohort study of cancer among benzene-exposed workers in China. Benzene Study Group. Environ Health Perspect. 1996a; 104:1339–41.

Yin S, Hayes R, Linet M, et al. A cohort study of cancer among benzene-exposed workers in China: overall results. Am J Ind Med. 1996b; 29:227–35.

Zou H. Henzel W, Liu S, Lutschg A, Wang X. Apaf-1, a human protein homologous to C. elegans CED-4, participates in cytochrome *c*-dependent activation of caspase-3. Cell. 1997;90:405–13.

Address for correspondence: Cyprian.V. Weaver, Department of Public Health, College of Medicine, Fu Jen University, 510 Chung Cheng Road, Hsinchuang, Taipei Hsien, Taiwan, 24205, R.O.C

E-mail: cyprianweaver@Yahoo.com